Omnidirectional bandgaps in Fibonacci quasicrystals containing single-negative materials

2010 J. Phys.: Condens. Matter 22 055403

(http://iopscience.iop.org/0953-8984/22/5/055403)

J. Phys.: Condens. Matter **22** (2010) 055403 (5pp) doi:10.1088/0953-8984/22/5/055403

Omnidirectional bandgaps in Fibonacci quasicrystals containing single-negative materials

Xin-Hua Deng[1,2,4], Jiang-Tao Liu[1], Jie-Hui Huang[1], Liner Zou[1] and Nian-Hua Liu[3]

[1] School of Science, Nanchang University, Nanchang 330031, People's Republic of China
[2] State Key Laboratory of Millimeter Waves, Southeast University, Nanjing 210096, People's Republic of China
[3] Institute for Advanced Study, Nanchang University, Nanchang 330031, People's Republic of China

E-mail: xhdengxh@yahoo.com.cn

Received 8 October 2009, in final form 17 December 2009
Published 15 January 2010
Online at stacks.iop.org/JPhysCM/22/055403

Abstract
The band structure and bandgaps of one-dimensional Fibonacci quasicrystals composed of epsilon-negative materials and mu-negative materials are studied. We show that an omnidirectional bandgap (OBG) exists in the Fibonacci structure. In contrast to the Bragg gaps, such an OBG is insensitive to the incident angle and the polarization of light, and the width and location of the OBG cease to change with increasing Fibonacci order, but vary with the thickness ratio of both components, and the OBG closes when the thickness ratio is equal to the golden ratio. Moreover, the general formulations of the higher and lower band edges of the OBG are obtained by the effective medium theory. These results could lead to further applications of Fibonacci structures.

(Some figures in this article are in colour only in the electronic version)

1. Introduction

Since the first experimental verification of a negative index of refraction [1], artificially constructed metamaterials have become of considerable interest, because these materials can exhibit electromagnetic characteristics unlike those of any conventional materials. There are mainly two kinds of metamaterials: double-negative (DNG) metamaterials whose permittivity (ε) and permeability (μ) are simultaneously negative [2, 3] and single-negative (SNG) metamaterials [4–6], which include the mu-negative (MNG) materials with negative μ but positive ε and the epsilon-negative (ENG) materials with negative ε but positive μ. Theoretical and experimental studies on the propagation of light through period structures containing SNG materials have evidenced the existence of a zero effective phase gap which is omnidirectional and insensitive to disorder [7–9].

Quasicrystals are some kind of non-periodic structures which lack long-range translational symmetry, but possess a certain orientation order. The structural ordering of quasicrystals is between the periodic and disordered systems [10]. Among quasicrystals the most studied are structures based on the Fibonacci sequence. Both classical and quantum waves in these structures have been shown to have a self-similar energy spectrum [11], a pseudo-bandgap corresponding to regions of forbidden frequencies [12], and critically localized states whose wavefunctions are characterized by power law asymptotes and self-similarity [13]. All these properties are typical for quasi-periodic structures so that Fibonacci superlattices are considered as archetypal structures to study the fundamental aspects of wave propagation in quasicrystals. Recently, the bandgaps of Fibonacci photonic crystals with DNG materials have been presented [14–16], and it has been found that the change in the width and location of the omnidirectional zero-$\bar{n}$ gap is limited when Fibonacci order is changed [16].

In this paper, we introduce the SNG materials into Fibonacci structure to study the bandgaps and band edges of Fibonacci structure. We show that a new type of OBG exists in the Fibonacci structures. In contrast to the Bragg gaps,

[4] Author to whom any correspondence should be addressed.

such an OBG is insensitive to the incident angle and both polarizations of light, and the width and location of the OBG do not change with Fibonacci order, but vary with the thickness ratio of the two media, and the OBG closes at the golden ratio point. Moreover, based on effective medium theory, the general formulations of the higher and lower band edges of the OBG are obtained.

2. Theoretical model and numerical method

The system under consideration is composed of two layers A and B stacked alternately along the z direction and following the rules of the Fibonacci sequence, that is, the nth order Fibonacci chain is obtained according to the concatenation rule $S_n = S_{n-1}S_{n-2}$, with the first two chains as $S_0 = \mathrm{B}$ and $S_1 = \mathrm{A}$. In this study, layers A and B represent ENG materials with thickness d_A and MNG materials with thickness d_B, respectively. ENG and MNG materials are assumed to be isotropic. Here, we use the Drude model to describe the SNG materials, that is

$$\varepsilon_\mathrm{A} = \varepsilon_a - \omega_{\mathrm{ep}}^2/(\omega^2 + \mathrm{i}\Gamma\omega), \qquad \mu_\mathrm{A} = \mu_a \tag{1}$$

in the ENG materials; and

$$\varepsilon_\mathrm{B} = \varepsilon_b, \qquad \mu_\mathrm{B} = \mu_b - \omega_{\mathrm{mp}}^2/(\omega^2 + \mathrm{i}\Gamma\omega) \tag{2}$$

in the MNG materials. Where ω_{ep} and ω_{mp} are the electronic plasma frequency and the magnetic plasma frequency, respectively; Γ is for the damping factors that contribute to the absorption and losses [17, 18]. These kinds of dispersion for A and B may be realized in special microstrips [19, 20].

The wave is incident from the vacuum to the nth order Fibonacci multilayer with incident angle θ. For the transverse electric (TE) wave, the electric field $\boldsymbol{E}$ is polarized along the y direction, the dielectric layers are parallel to the x–y plane. In general, the electric and magnetic fields at any two positions z and $z + \Delta z$ in the same layer are connected via a transfer matrix [21, 22]

$$M_j(\Delta z, \omega) = \begin{pmatrix} \cos(k_z^j \Delta z) & \mathrm{i}\frac{1}{q_j}\sin(k_z^j \Delta z) \\ \mathrm{i}q_j \sin(k_z^j \Delta z) & \cos(k_z^j \Delta z) \end{pmatrix}, \tag{3}$$

where $k_z^j = (\omega/c)\sqrt{\varepsilon_j}\sqrt{\mu_j}\sqrt{1 - \sin^2\theta/\varepsilon_j\mu_j}$ is the z component of the wavevector k^j in the jth layer, c is the speed of light in a vacuum, and $q_j = \sqrt{\varepsilon_j}/\sqrt{\mu_j}\sqrt{1 - (\sin^2\theta/\varepsilon_j\mu_j)}$ is the component of the wavevector along the interface. The transmission and reflection coefficient $t(\omega, \theta)$ and $r(\omega, \theta)$ can be expressed as

$$t(\omega, \theta) = \frac{2\cos\theta}{(x_{11} + x_{22})\cos\theta + \mathrm{i}(x_{12}\cos^2\theta - x_{21})}, \tag{4}$$

$$r(\omega, \theta) = \frac{(x_{22} - x_{11})\cos\theta + \mathrm{i}(x_{12}\cos^2\theta + x_{21})}{(x_{11} + x_{22})\cos\theta + \mathrm{i}(x_{12}\cos^2\theta - x_{21})}. \tag{5}$$

Here $x_{ij}(i, j = 1, 2)$ is the matrix element of X_n which represents the total transfer matrix of the nth order Fibonacci sequence. The X_n can be deduced from the following recursion relations:

$$X_n = X_{n-1}X_{n-2} \qquad (n \geqslant 2) \tag{6}$$

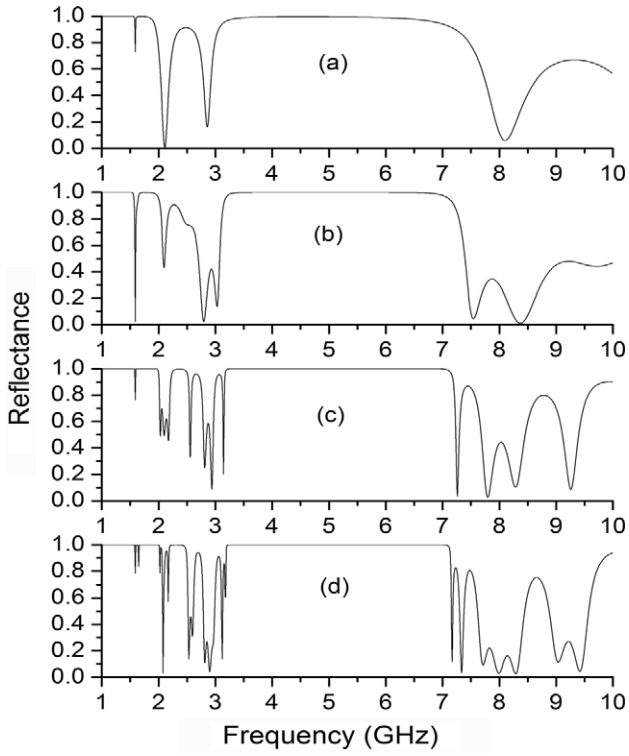

Figure 1. Normal incidence reflection spectra for the different order Fibonacci structures as a function of the angular frequency with (a) S_6, (b) S_7, (c) S_8, and (d) S_9.

with

$$X_0 = M_\mathrm{B}(d_\mathrm{B}, \omega), \qquad X_1 = M_\mathrm{A}(d_\mathrm{A}, \omega). \tag{7}$$

The transverse magnetic (TM) wave can be treated in a similar way. In the following calculations, we first considered the lossless SNG materials (i.e. $\Gamma = 0$ in equations (1) and (2)) in the microwave frequency range; we choose $\varepsilon_a = \mu_b = 1$, $\mu_a = \varepsilon_b = 3$, $\omega_{\mathrm{ep}} = \omega_{\mathrm{mp}} = 10$ GHz.

3. Results and discussion

First, we choose $d_\mathrm{A} = 12$ mm and $d_\mathrm{B} = 6$ mm to study the reflection spectra for higher order ($n \geqslant 6$) Fibonacci quasicrystals. In figure 1, the reflection spectra for normal incidence are shown in the cases of Fibonacci structures where S_6 (figure 1(a)), S_7 (figure 1(b)), S_8 (figure 1(c)), and S_9 (figure 1(d)). It can be seen from figure 1 that, with increasing order of Fibonacci structures, a large reflectance band centered at the angular frequency of 5.24 GHz remains invariant and the edges of the reflectance band become much sharper. In fact, the reflectance band can occur in all higher-order Fibonacci structures. For simplicity, others are not given in this paper.

Next, we analyze the formation mechanism of the reflectance band in Fibonacci structures based on effective medium theory. For the nth-order Fibonacci structure, the general average ε and μ can be written as

$$\langle\varepsilon\rangle_n = \frac{N_\mathrm{A}^n d_\mathrm{A}\varepsilon_\mathrm{A} + N_\mathrm{B}^n d_\mathrm{B}\varepsilon_\mathrm{B}}{N_\mathrm{A}^n d_\mathrm{A} + N_\mathrm{B}^n d_\mathrm{B}}, \tag{8}$$

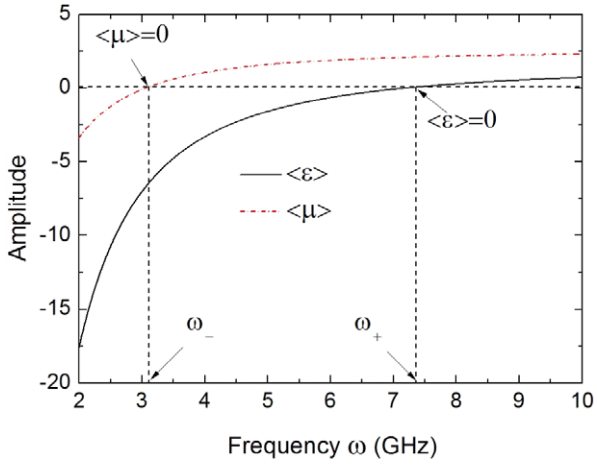

Figure 2. The curves of the amplitude of average permittivity and average permeability versus the angular frequency with $d_A = 6$ mm and $d_B = 3$ mm.

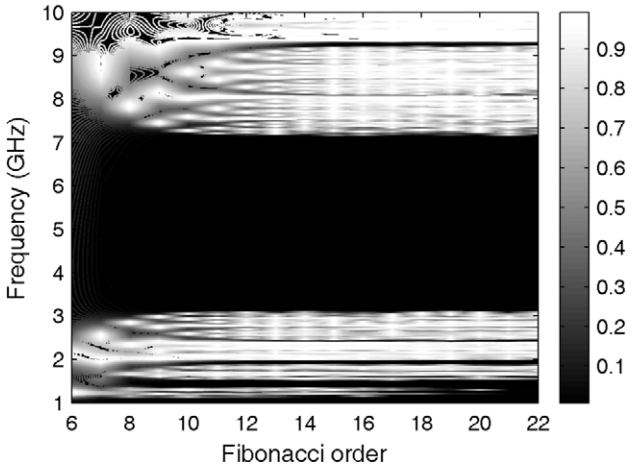

Figure 3. The photonic spectrum of Fibonacci lattices as a function of the Fibonacci order with $d_A = 6$ mm and $d_B = 3$ mm.

$$\langle\mu\rangle_n = \frac{N_A^n d_A \mu_A + N_B^n d_B \mu_B}{N_A^n d_A + N_B^n d_B}, \tag{9}$$

where N_A^n and N_B^n represent the number of layers of the ENG and MNG materials in the nth-order Fibonacci structure, respectively. According to the recursion rules of Fibonacci structures, the number of layers in S_n is the Fibonacci number F_{n+1}, where $F_1 = 1$, $F_2 = 1$, and $F_{n+1} = F_{n-1} + F_n$. The number of layers of type A(B) in S_n is the Fibonacci number $F_n(F_{n-1})$, namely, $N_A^n = F_n$ and $N_B^n = F_{n-1}$. Then equations (8) and (9) can be simplified as

$$\langle\varepsilon\rangle_n = \frac{F_n d_A \varepsilon_A + F_{n-1} d_B \varepsilon_B}{F_n d_A + F_{n-1} d_B}, \tag{10}$$

$$\langle\mu\rangle_n = \frac{F_n d_A \mu_A + F_{n-1} d_B \mu_B}{F_n d_A + F_{n-1} d_B}. \tag{11}$$

A very important property of the Fibonacci numbers involves the quotient $\tau_n = F_n/F_{n-1}$ with $\lim_{n\to\infty} \tau_n = \tau = (1+\sqrt{5})/2 = 1.618$. Equations (10) and (11) can be simplified as

$$\langle\varepsilon\rangle_n = \frac{\tau_n d_A \varepsilon_A + d_B \varepsilon_B}{\tau_n d_A + d_B}, \tag{12}$$

$$\langle\mu\rangle_n = \frac{\tau_n d_A \mu_A + d_B \mu_B}{\tau_n d_A + d_B}. \tag{13}$$

For infinite-order ($n \to \infty$) Fibonacci structures, in fact, for higher-order ($n \geqslant 9$) Fibonacci structures, $\tau_n \approx \tau = (1+\sqrt{5})/2$, equations (12) and (13) can be simplified as

$$\langle\varepsilon\rangle = \frac{\tau d_A \varepsilon_A + d_B \varepsilon_B}{\tau d_A + d_B} = \frac{\tau \varepsilon_A + \varepsilon_B d_B/d_A}{\tau + d_B/d_A}, \tag{14}$$

$$\langle\mu\rangle = \frac{\tau d_A \mu_A + d_B \mu_B}{\tau d_A + d_B} = \frac{\tau \mu_A + \mu_B d_B/d_A}{\tau + d_B/d_A}. \tag{15}$$

Figure 2 shows the curves of $\langle\varepsilon\rangle$ and $\langle\mu\rangle$ versus the angular frequency ω with $d_A = 6$ mm and $d_B = 3$ mm. It is shown that when the angular frequency is between $\omega_- = 3.11$ GHz (corresponding to the zero point of $\langle\mu\rangle$) and $\omega_+ = 7.37$ GHz (corresponding to the zero point of $\langle\varepsilon\rangle$), $\langle\mu\rangle$ is greater than zero and $\langle\varepsilon\rangle$ is less than zero. So the refractive index of the effective medium is imaginary. Hence, the effective medium does not allow the propagation of the electromagnetic wave, and the corresponding frequency range $\Delta\omega = \omega_+ - \omega_- = 4.26$ GHz should be a gap in the structure. This gap is regarded as an SNG gap. So the higher and lower edges of the SNG gap can be determined by $\langle\varepsilon\rangle = 0$ and $\langle\mu\rangle = 0$. From equations (14) and (15), we can seen that, keeping the ratio of d_B/d_A constant and increasing the values of d_A and d_B simultaneously, equations (14) and (15) are invariant, ω_- (the root of $\langle\mu\rangle = 0$) and ω_+ (the root of $\langle\varepsilon\rangle = 0$) remain constant. So the gap width is invariant to scaling.

For comparison, we plot the photonic spectrum of Fibonacci lattices as a function of the Fibonacci order with $d_A = 6$ mm and $d_B = 3$ mm in figure 3. We can see from figure 3 that, when changing Fibonacci order n from 6 to 9, the higher edge of the SNG gap shifts down to lower frequencies, while the lower edge of the SNG gap shifts up to higher frequencies, and the frequency width becomes less. While changing the Fibonacci order n from 9 to 22, the higher and lower edges of the SNG gap remain constant, the frequency region of the SNG gap runs from 3.11 to 7.37 GHz and the frequency width is 4.26 GHz. So, numerical results are identical to those in figure 2 based on effective medium theory for higher-order ($n \geqslant 9$) Fibonacci structures.

In order to investigate the higher and lower edges of the SNG gap in Fibonacci lattices, we plot the curves of $\langle\varepsilon\rangle = 0$ and $\langle\mu\rangle = 0$ versus the angular frequency ω for various d_B/d_A in figure 4. It is shown that the SNG gap becomes larger as the thickness ratio of the two media moves further away from the golden ratio (i.e. 1.618), and closes as the thickness ratio becomes equal to the golden ratio. Both $\langle\varepsilon\rangle$ and $\langle\mu\rangle$ are equal to zero at the golden ratio point, which corresponds to the phase-match (at wave impedance matching frequency) case, and no gap exists around the zero effective phase delay point. While the phase of ENG and MNG materials does not match when the d_B/d_A value is not equal to the golden ratio,

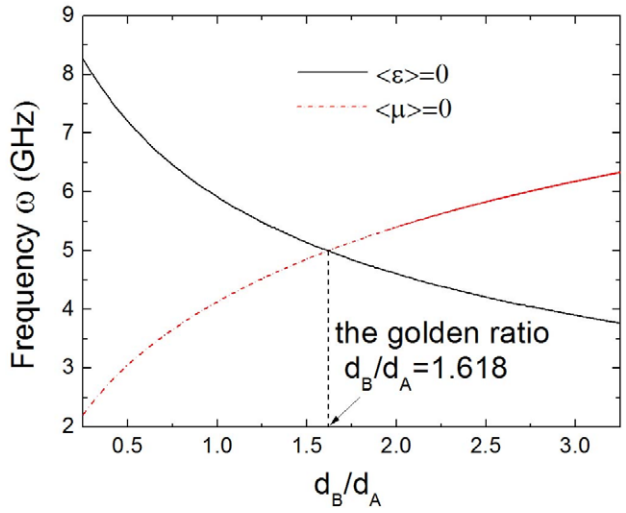

Figure 4. The SNG gap profile of Fibonacci lattices as a function of the ratio d_B/d_A.

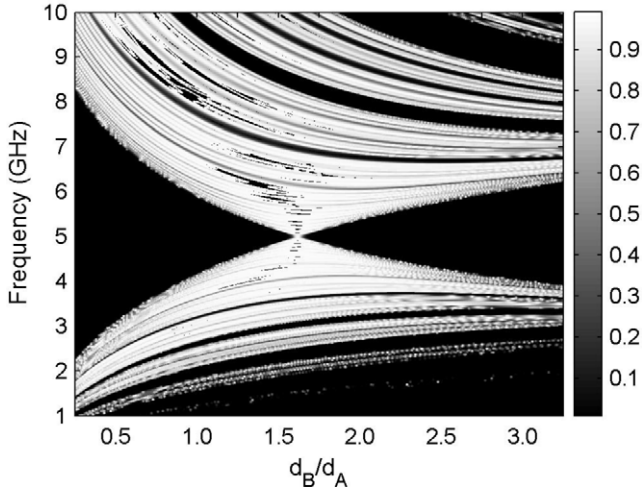

Figure 5. The photonic spectrum of Fibonacci lattices S_{13} as a function of the ratio d_B/d_A.

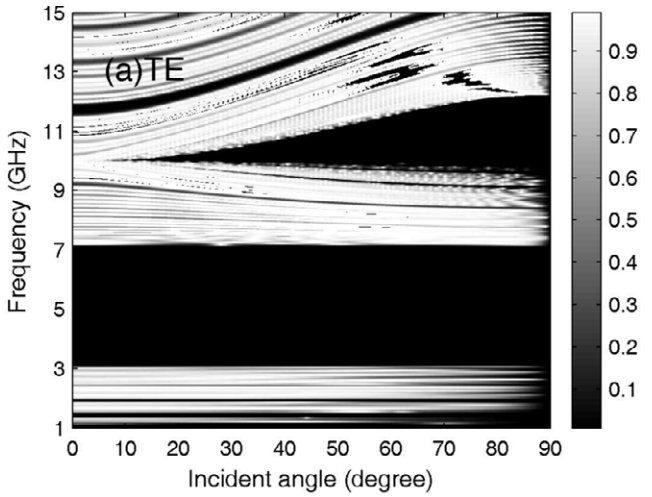

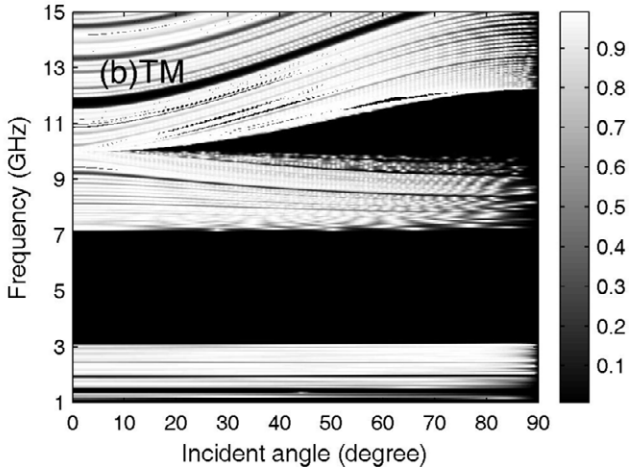

Figure 6. Frequency bandgaps of Fibonacci lattices S_{13} with $d_A = 6$ mm and $d_B = 3$ mm for different incident angles and polarizations: (a) TE and (b) TM polarization.

mismatch will cause a gap in Fibonacci lattices, and the further away from the golden ratio the d_B/d_A value is, the larger the mismatch of the phase and the larger the SNG gap. Moreover, the lower and upper edges of the SNG gap are affected by the thickness ratio, i.e. the lower edge of the SNG gap shifts to lower frequencies, while the upper edge of the SNG gap shifts to higher frequencies when the thickness ratio of the two media is far away from the golden ratio.

For comparison, we plot the photonic spectrum of Fibonacci lattices as a function of the ratio d_B/d_A in figure 5. It is shown that, when changing d_B/d_A from 0.25 to the golden ratio (i.e. 1.618), the SNG gap becomes larger, while changing d_B/d_A from 1.618 to 3.25, the SNG gap becomes less. Namely, the SNG gap becomes larger when the thickness ratio of the two media is far away from the golden ratio. When d_B/d_A is equal to the golden ratio, Fibonacci structures become transparent around the frequency point. These results are identical to those in figure 4.

Next, we discuss the band structure of Fibonacci lattices for different incident angle and polarization of light. We take S_{13} as an example and investigate the wide angle reflectance behavior of the system. In figure 6, we show transmittance spectra for both TE (figure 6(a)) and TM (figure 6(b)) polarizations versus angular frequency for different incident angles. When the incident angle increases from 0° to 90°, the higher and lower edges of the SNG gap of Fibonacci lattices remain invariant for both polarizations. It can be seen that the band edges of the SNG gap of the Fibonacci lattices are insensitive to the incident angle and the polarization of light, such an SNG gap is omnidirectional. So the frequency range of the OBG for both polarizations is between 3.11 and 7.37 GHZ and the frequency width is 4.26 GHz. This property is different from the zero-$\bar{n}$ gap mechanisms in Fibonacci structures containing left-handed materials [16], in which the lower or upper frequency edges of the zero-$\bar{n}$ gap are sensitive to incident angle for different polarizations, and are different fundamentally from those of OBGs in Fibonacci dielectric superlattices [23], in which OBGs depend only on TM polarization. The main reason for the different

results is because their mechanisms of band formation are different. The band formation comes from light scattering of propagating modes in Fibonacci dielectric superlattices; while for Fibonacci structures with SNG materials, it originates from light tunneling of evanescent modes.

It should be pointed out that the loss of SNG materials cannot be neglected, though the imaginary part of the permittivity or permeability at some frequencies is very low. The main properties of the OBG in Fibonacci photonic crystals, however, are not affected because the band edges of the OBG determined by equations (14) and (15) do not present any rapid change when a very small loss is added to the SNG materials. The losses only decrease the transmission intensity.

4. Conclusions

In summary, the band structure and bandgaps of one-dimensional quasicrystals composed of ENG materials A and MNG materials B, arranged according to a recursion rule of the Fibonacci type, have been studied. We have proven that certain combinations of both components can lead to the formation of an OBG, which is insensitive to the incident angle and the polarization of light. In fact this OBG ceases to change with increasing Fibonacci order and it only varies with the thickness ratio of both components. The OBG closes when the thickness ratio is equal to the golden ratio. Moreover, based on effective medium theory, the higher and lower edges of the OBG can be determined by $\langle\varepsilon\rangle = 0$ and $\langle\mu\rangle = 0$. These results could lead to further applications of the Fibonacci structures.

Acknowledgments

This work is supported by the Open Research Fund of State Key Laboratory of Millimeter Waves (grant no. K200901), the National Natural Science Foundation of China (grant nos 10904059, 10804042 and 10664002), the Natural Science Foundation of Jiangxi Province (grant no. 2008GZW0003), the Science and Technology Project of the Education Department of Jiangxi Province (grant no. GJJ09073), and PCSIRT from China (grant no. IRT0730).

References

[1] Shelby R A, Smith D R and Schultz S 2001 *Science* **292** 77
[2] Veselago V G 1968 *Sov. Phys.—Usp.* **10** 509
[3] McCall M W, Lakhtakia A and Weiglhofer W S 2002 *Eur. J. Phys.* **23** 353
[4] Deng X H and Liu N H 2009 *J. Phys. D: Appl. Phys.* **42** 045420
[5] Xiang Y J, Dai X Y, Wen S C and Fan D Y 2007 *J. Opt. Soc. Am.* A **24** 28
[6] Chen Y H, Dong J W and Wang H Z 2006 *Appl. Phys. Lett.* **89** 141101
[7] Jiang H T, Chen H, Li H Q, Zhang Y W, Zi J and Zhu S Y 2004 *Phys. Rev.* E **69** 066607
[8] Wang L G, Chen H and Zhu S Y 2004 *Phys. Rev.* B **70** 245102
[9] Zhang L W, Zhang Y W, He L, Li H Q and Chen H 2006 *Phys. Rev.* E **74** 056615
[10] Fujiwara T and Ogawa T 1990 *Quasicrystals* (Heidelberg: Springer)
[11] Gumbs G and Ali M K 1988 *Phys. Rev. Lett.* **60** 1081
[12] Nori F and Rodriguez J P 1986 *Phys. Rev.* B **34** 2207
[13] Fujiwara T, Kohmoto M and Tokihiro T 1989 *Phys. Rev.* B **40** 7413
[14] Vasconcelos M S, Mauriz P W, de Medeiros F F and Albuquerque E L 2007 *Phys. Rev.* B **76** 165117
[15] Bruno-Alfonso A, Reyes-Gómez E, Cavalcanti S B and Oliveira L E 2008 *Phys. Rev.* A **78** 035801
[16] Hsueh W J, Chen C T and Chen C H 2008 *Phys. Rev.* A **78** 013836
[17] O'Brien S and Pendry J B 2002 *J. Phys.: Condens. Matter* **14** 6383
[18] Pendry J B and Smith D R 2004 *Phys. Today* **57** 37
[19] Eleftheriades G V, Iyer A K and Kremer P C 2002 *IEEE Trans. Microw. Theory Tech.* **50** 2702
[20] Zhang L W, Zhang Y W, He L, Li H Q and Chen H 2006 *Phys. Rev.* E **74** 056615
[21] Born M and Wolf E 1999 *Principles of Optics* 7th edn (Oxford: Cambridge University Press)
[22] Yeh P 1988 *Optical Waves in Layered Media* (New York: Wiley)
[23] Lusk D and Placido F 2005 *Thin Solid Films* **492** 226